https://doi.org/10.5194/egusphere-2026-241
Preprint. Discussion started: 4 March 2026

Saturation effect of background temperature and aridity on vegetation phenology sensitivity to urban warming

Zhang Zhenzhen[1*], Zhang Yongqi[1], Cui Shufen[2], Sun Liheng[3], Lin Xingwen[1], Wu Chaofan[1], Zhang Zhaoyang[1], Chen Yuanjian[1], Wen Qingqing[4]

[1]College of Geography and Environmental Sciences, Zhejiang Normal University, Jinhua 321004, China

[2]College of Business, Lishui University, Lishui 323200, China

[3]Faculty of Management, Universiti Teknologi Malaysia, Johor Bahru 81310, Malaysia

[4]The Administration Center of Jinhua Wucheng Nanshan Provincial Nature Reserve, Jinhua 321000, China

*** Correspondence: Zhang Zhenzhen (zhangzhen@zjnu.cn)**

Societal Impact Statement

As cities grow and climates warm, the Urban Heat Island (UHI) effect increasingly alters urban ecosystems. This study analyzed 293 Chinese cities to reveal how baseline temperature and aridity shape vegetation's response to UHI. We found a "saturation effect," where UHI's impact weakens under certain background conditions. This helps explain why urban greening outcomes vary regionally. Our findings offer new insight into urban ecology and can support climate-smart planning, helping cities adapt more effectively and sustainably.

Abstract:

In this study, urban warming effects on vegetation phenology were assessed for 293 cities in China. The variations in urban warming effects were expected to be attributed to the baseline land surface temperature (LST) and the aridity index (AI) of each locale. LST and AI related phenology and their temperature sensitivity ($R_{t\text{-}SOS}$

https://doi.org/10.5194/egusphere-2026-241
Preprint. Discussion started: 4 March 2026

and $R_{t\text{-}EOS}$) was quantified. We observed an urban-rural phenological disparity of 12.06 days for Start of Season (ΔSOS) and 9.86 days for End of Season (ΔEOS) among the studied cities. Spatially, cities in high latitude regions and coastal areas exhibited pronounced negative ΔSOS shifts and positive ΔEOS shifts, positively correlating with $R_{t\text{-}SOS}$ and $R_{t\text{-}EOS}$, respectively. Employing a continent-wide preseason temperature (T), we observed a logistic decrease for SOS and an increase for EOS, illustrating the "saturated effect" of warming on plant phenology-patterns echoed within urban settings. First-order derivatives of those logistic curves identified a highest phenological sensitivity at T=4℃ and T=6℃, as well as the warming benefit range of -3.5℃-10℃ and 2℃-14℃ for SOS and EOS respectively. Substituting T with LST, weaker ΔSOS and ΔEOS would be presented in warmer regions only when LST exceeded 12.5℃ and 4℃ for spring and autumn, respectively. Except for LST, AI exhibited a positive correlation with ΔSOS and $\Delta R_{t\text{-}SOS}$, but a negative one with ΔEOS and $\Delta R_{t\text{-}EOS}$. Collectively, LST and AI explained 75.05% and 76.21% of the phenological variance across the continent for ΔSOS and ΔEOS, respectively. These findings lay the groundwork for predicting vegetation changes under global warming at large scales.

Keywords：urbanization; heat island effect; vegetation phenology sensitivity; aridity index; land surface temperature; “saturation effect”

1. Introduction

Vegetation phenology, a critical aspect of ecosystem dynamics, exhibits significant sensitivity to climate variations(Badeck et al., 2004). Recent investigations have highlighted the influence of urban warming phenomena in precipitating earlier onset of green-up phases (SOS) and postponing the transition to dormancy (EOS)(Jeonget et al., 2019; Meng et al., 2020; Qiu et al., 2020; Zhou et al., 2016). The cascading effects of these shifts extend beyond mere phenological alterations, contributing to a spectrum of ecological and environmental challenges(Zhou et al., 2016; Qiu et al., 2017; Tang et al., 2017) .

However, the degree to which warming benefits phenological changes has been

https://doi.org/10.5194/egusphere-2026-241
Preprint. Discussion started: 4 March 2026

widely debated(Chmielewski & Rötzer, 2001; Ding et al., 2020; Yao et al., 2017). Studies have argued that background temperature heterogeneity has the potential to disrupt phenology responses to urban warming(Meng et al., 2020). For example, in cold high-latitude regions of the Northern Hemisphere, more advanced SOS and delayed EOS has been reported in response to warming events(Meng et al., 2020; Qiu et al., 2020; Dallimer et al., 2016; Gazal et al., 2008; Li et al., 2021). While these studies offer empirical evidence, they do not sufficiently elucidate the underlying cause and its quantifiable relationship.

Differences in plant phenological sensitivity to background temperatures might contribute to the spatial heterogeneity of plant responses to urbanization(Meng et al., 2020). In the field of biology, “saturation effects” refer to the psychological phenomenon where the efficacy of a stimulus declines due to the continuous application of the same stimulus material. Similarly, in the field ecology, according to the theory of tolerance curves, an organism's physiological functions enhance with increasing environmental factors, reaching a point of physiological saturation, beyond which no further enhancement occurs and a decline may ensue(Ketola & Kristensen, 2017). For example, many studies had argued that the plant physiological processes such as photosynthesis, respiration, transpiration etc. would not increase linearly with increased temperature(Sage & Kubien, 2007; Ge et al., 2021). On the contrary, they will gradually slow down, and even decreased when temperature surpass a threshold(Sage & Kubien, 2007; Mathur et al., 2021). A meta-analysis of the response of above-ground plant growth to experimental ecosystem warming had proved a greater positive response to warming in colder ecosystems(Rustad et al., 2001). Since the warmer regions have higher mean temperature, thus we expected that their urban warming related benefits for phenology (i.e., advanced SOS and delayed EOS) will also gradually approaching the saturated point. Extra warming due to urban warming effect will not promoted the advancement of SOS and delay of EOS, i.e., the “saturation effect”. However, these theories are still need to verified.

It is noteworthy that except for background temperature, drought conditions can passively disrupt phenological responses linked to ambient temperature(Peng et al.,

https://doi.org/10.5194/egusphere-2026-241
Preprint. Discussion started: 4 March 2026

2019; Yuan et al., 2020). For spring phenology, drought induces the accumulation of abscisic acid (ABA)(Mcadam, 2013), leading to delayed spring germination(Eidt & Little, 1968). A pronounced delayed SOS was documented on the Yungui Plateau preceding drought occurrences(Peng et al., 2019). Likewise, delayed SOS resulting from drought was also observed in grassland ecosystems in Northeastern China(Yuan et al., 2020). Laboratory investigations have demonstrated that one-year-old saplings of Pedunculate oak exhibit delayed bud burst following a one-year drought treatment(Čehulić et al., 2019). Concerning autumn phenology, drought conditions prior to the season can trigger protein degradation and impair chloroplast function(Ge et al., 2021; Shi et al., 2014), potentially leading to widespread crown defoliation(Pollastrini et al., 2017). Consequently, under drought stress conditions, early dormancy (advanced EOS) is anticipated due to heightened water stress(Wang et al., 2020). Therefore, it is reasonable to anticipate that the sensitivity of phenology will be compromised in drought-affected regions, thereby diminishing the positive impact of warming on phenological responses.

As a developing country with diverse climates and rapid urbanization across its vast territory, China is confronted with significant challenges stemming from the urban heat island effect(He et al., 2017). The intensity of this effect averages at 0.9 ± 1.1 ℃, although it exhibits considerable variation among different regions(Li et al., 2021). Thus, an investigation into the phenological response of plants to urbanization in China would enhance our understanding of their ability to acclimate to climate changes across various environments.

The primary objectives of this study encompassed the following: (1) exploring the spatial distribution of plant phenological responses to the urban heat island effect throughout mainland China; (2) quantify the saturation effect caused by the spatial variability of phenological responses correlated with background temperature across the cold-hot gradient; and (3) assessing whether the benefits of urban warming would be counteracted in drought-affected areas.

https://doi.org/10.5194/egusphere-2026-241
Preprint. Discussion started: 4 March 2026

2. Materials and Methods

2.1 Study Area

In our study, we conducted an analysis covering a total of 293 prefecture-level cities in China (excluding Taiwan, Autonomous Prefecture, and regions), taking into account the data from the year 2020 (http://xzqh.mca.gov.cn/map) (Figure 1). It was hypothesized that the urban warming effect is most pronounced in urban centers and gradually diminishes towards rural areas(Zhang et al., 2004). To determine the urbanization intensity of each city, nighttime light data from NPP-VIIRS (Table 1) was utilized, employing the reference comparison method. The optimal segmentation threshold was established based on the statistical yearbook(Fan et al., 2019). Moreover, urban built-up areas were identified using the comparison method and annual average data derived from NPP-VIIRS night lights between 2013 and 2020. All data processing procedures were performed using ArcGIS 10.2. A total of ten buffer zones were created within a radius of 20 kilometers from the city center, with each buffer zone set at a distance of 2 kilometers from the center (Figure 1).

https://doi.org/10.5194/egusphere-2026-241
Preprint. Discussion started: 4 March 2026

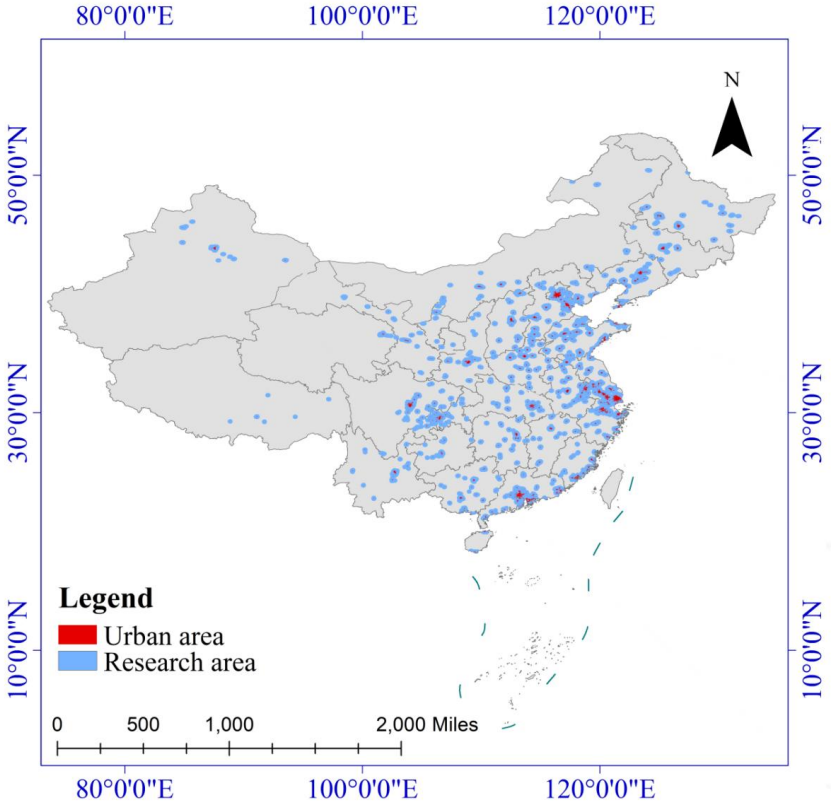

Figure 1. City centers (red area) and buffer zones (blue area) of the 293 prefecture-level cities in China. The map, generated using ArcGIS – version 10.2 (https://www.esri.com/about/newsroom/arcwatch/the-best-of-arcgis-10-2/), features administrative boundaries sourced from the Ministry of Civil Affairs of the People's Republic of China (http://xzqh.mca.gov.cn/map).Source: Esri, TomTom, FAO, USGS, and the GIS User Community; Ministry of Civil Affairs of the People's Republic of China | Powered by Esri.

2.2 Vegetation phenology extraction

Phenology data spanning the years 2010 to 2020 was derived from MODIS Enhanced Vegetation Index (EVI) 16-day composite data with a spatial resolution of 250m (MOD13Q1) and processed utilizing TIMESAT. To mitigate challenges such as cloud cover and snow, the raw EVI time series dataset underwent smoothing through an S-G filter method(Cai et al., 2017). Subsequently, a dynamic threshold technique

https://doi.org/10.5194/egusphere-2026-241
Preprint. Discussion started: 4 March 2026

was employed to extract the phenology data, utilizing a seasonal amplitude of 20%, a parameter proven effective for phenology extraction in urban environments5,31-33(Zhou et al., 2016; Buyantuyev & Wu, 2012; Cong et al., 2012; White et al., 2009). The datasets underwent preprocessing to eliminate pixels with minimal vegetation EVI, such as bodies of water and fully paved surfaces. To ensure the exclusion of unrealistic values for the start of season (SOS) and end of season (EOS), a range of 30 to 180 days and 210 to 360 days was specified. Contingent upon previous studies(Zhou et al., 2016; Zhang et al., 2006). Efforts were made to reduce the impact of outlier years by averaging the phenology data for each pixel across the timeframe from 2010 to 2020.

Furthermore, we employed land cover data from the MCD12Q1 dataset, which boasts a 500-meter resolution, to mitigate the impact of agricultural practices on the mainland during our analysis. The MCD12Q1 dataset categorizes land into 17 distinct classes. These include various types of forested areas such as Evergreen Coniferous Forests, Deciduous Needle-leaf Forests, Evergreen Broad-leaf Forests, Deciduous Broad-leaf Forests, Mixed Forests, as well as Closed Shrub lands, Open Shrub lands, Savannas, woody savannas, Grasslands, and Croplands.

Given the frequent human-induced disturbances in Croplands in the rural regions and the regular manual pruning of Grasslands in the urban center, Savannas, woody savannas, Grasslands, and Croplands were excluded from our study. The remaining land types were consolidated into broader categories: Broad-leaf Forests (BF), which encompasses both Deciduous and Evergreen Broad-leaf Forests; Coniferous Forests (CF), comprising both Deciduous and Evergreen Coniferous Forests; Mixed Forests; and Shrubs, which includes both Closed and Open Shrublands. This classification approach allowed us to focus our analysis on land types that are less influenced by human activities.

Table1 Data inventory used in this study

Data type	Resolution	Layer	Data sources	Year
MOD13Q1	250m/16d	EVI	https://search.earthdata.nasa.gov	2010-2020

https://doi.org/10.5194/egusphere-2026-241
Preprint. Discussion started: 4 March 2026

MOD11A2	1000m/8d	LST_Day LST_Night	https://search.earthdata.nasa.gov	2010-2020
MOD16A2	500m/8d	PET	https://search.earthdata.nasa.gov	2010-2020
MCD12Q1	500m	Land Cover	https://search.earthdata.nasa.gov	2010-2020
VIIRS	500m	yearly average	https://eogdata.mines.edu	2013-2020
Precipitation data	1000m	monthly average	http://www.geodata.cn	2010-2020
China's urban zoning data			https://www.resdc.cn	2020
Station climates		monthly average	(http://data.cma.cn/en	2010-2020

2.3 Pre-season temperature and background climates

Building upon the methodology of a previous study(Piao et al., 2006), the pre-season temperature (T) was characterized as the mean temperature for the three months preceding the onset of the phenological season. For alignment with the phenology information, the average temperature dataset was resampled to a 250m resolution using the nearest neighbor interpolation technique. To evaluate the performance of the downscaling procedure, the observed long-term monthly Temperature and Precipitations across China were obtained from the National Meteorological Information Center of China (http://data.cma.cn/en). This dataset included observations from 496 national weather stations during 2010–2020. Upon conducting a fitting analysis with station data, we observed that the coefficient of determination (R^2) for monthly mean temperature and remote sensing data reached 0.93, while that for monthly precipitation and remote sensing data achieved 0.85. These results indicated that the downscaled meteorological data sufficiently meet the requirements of this study.

The background climates were evaluated utilizing land surface temperature (LST) and aridity index (AI) as indicators. The LST and AI data for each pixel were averaged over the temporal span from 2010 to 2020. Specifically, MODIS LST datasets exhibiting an absolute bias of less than 1K were selected as optimal for our

https://doi.org/10.5194/egusphere-2026-241
Preprint. Discussion started: 4 March 2026

investigation, in line with previous studies(Gow et al., 2016; Pablos et al., 2016; Qiao et al., 2013; Wan et al., 2008). Version-6 LST data sourced from Aqua MODIS (MOD11A2, 8-day composite, 1km spatial resolution, covering the period from 2010 to 2020) were employed in this analysis. Additionally, daily temperature (T) was calculated as the mean of daytime and nighttime temperatures, following the methodology outlined by Kang(Kang et al., 2016). AI was expressed as:

$$AI = PET/P \quad (1)$$

where, PET denotes the annual potential vapor transpiration, while P represents the annual precipitation. The PET values spanning from 2010 to 2020 were extracted from the MOD16A2 monthly synthetic product, characterized by an 8-day temporal resolution and a spatial resolution of 500 meters, as delineated in Table 1. The annual precipitation (P) dataset was derived from the monthly precipitation records of China encompassing the timeframe from 1901 to 2020, possessing a spatial resolution of 1 km. Subsequently, both PET and P datasets were resampled to a spatial resolution of 250 meters to facilitate the ensuing spatial analysis(Peng, 2020).

2.4 Urbanization effect on phenology

The phenology date of each vegetation was extracted in each buffer zone. Finally, the mean phenology in this buffer zone was weighted by the phenology of each vegetation types. To ensure comparability in phenological analyses across buffer zones, we first identify the common vegetation types present in all zones and exclude the non-shared ones. We then calculate the phenological means for these common types within each buffer zone and average these values to determine the overall mean vegetation phenology for the entire buffer region, as showed below (equation 2, 3).

$$SOS_i = \sum SOS_{ij}/n \quad (2)$$

$$EOS_i = \sum EOS_{ij}/n \quad (3)$$

SOS_i and EOS_i is the mean SOS and EOS of i-th buffer zone, SOS_{ij} and EOS_{ij} is the mean SOS and EOS of the j-th vegetation type in the i-th buffer zone. n is the number of the shared vegetation types in all the buffer zone.

To investigate the impact of urbanization on phenology, mean values of start of

https://doi.org/10.5194/egusphere-2026-241
Preprint. Discussion started: 4 March 2026

season (SOS) and end of season (EOS) in each buffer zone were analyzed the for the period between 2010 to 2020, and fitted with respect to their distance from the urban center. In this study, the outermost buffer zone and the urban center were defined as the rural region and the urban region, respectively, since SOS and EOS gradually decreases and approaches 0 at 15 km and beyond (Figure S1). Similar pattern was also observed for all the four vegetation types (Figure S2). As per prior investigations, the phenological sensitivity (R_t) to temperature was quantified by calculating the partial correlation coefficient between T and the phenology dates ($R_{t\text{-}SOS}$ and $R_{t\text{-}EOS}$)(Meng et al., 2020).

The difference of SOS_i and EOS_i between the urban and rural regions for the phenology dates were quantified. Since the change rates was approaching 0 at 15 km and beyond (Figure S2), The outermost buffer zone (20km away from the urban center) and the urban center were defined as the rural region and the urban region, respectively. The phenology difference of between urban and rural regions (ΔSOS and ΔEOS) was calculated as below:

$$\Delta SOS = SOS_{(0)} - SOS_{(10)} \quad (4)$$

$$\Delta EOS = EOS_{(0)} - EOS_{(10)} \quad (5)$$

Among which, SOS_0 and SOS_{10} is the mean SOS of the urban center and the 10-th buffer zone (20km away), EOS_0 and EOS_{10} is the mean EOS of the urban center and the 10-th buffer zone (20km away).

The R_t of SOS and EOS ($R_{t\text{-}SOS}$ and $R_{t\text{-}EOS}$) difference between the urban and rural regions was defined as below:

$$\Delta R_{t\text{-}SOS} = R_{t\text{-}SOS(0)} - R_{t\text{-}SOS(20)} \quad (6)$$

$$\Delta R_{t\text{-}EOS} = R_{t\text{-}EOS(0)} - R_{t\text{-}EOS(20)} \quad (7)$$

Among which, $R_{t\text{-}SOS(0)}$ and $R_{t\text{-}SOS(20)}$ is the mean $R_{t\text{-}SOS}$ of the urban center and the 10-th buffer zone (20km away), $R_{t\text{-}EOS(0)}$ and $R_{t\text{-}EOS(20)}$ is the mean $R_{t\text{-}EOS}$ of the urban center and the 10-th buffer zone (20km away).

2.5 Background climates determined phenology response

In order to elucidate the distinct impacts of LST and AI on urban and rural

https://doi.org/10.5194/egusphere-2026-241
Preprint. Discussion started: 4 March 2026

components, a partial correlation analysis was executed. Specifically, the average LST or AI values recorded from 2010 to 2020 for each of the 293 cities were correlated with their respective ΔSOS, ΔEOS, $\Delta R_{t\text{-}SOS}$, and $\Delta R_{t\text{-}EOS}$ values, while controlling for the influence of the other climatic factor.

This study employed path analysis (PCA) as a methodological approach to examine both the direct and indirect effects of background climate variables (LST and AI) on phenological responses (SOS and EOS), as well as their corresponding discrepancies (ΔSOS and ΔEOS) and rates of change ($\Delta R_{t\text{-}SOS}$ and $\Delta R_{t\text{-}EOS}$).

In the path analysis, we initially ascertained the model's congruence with empirical data by evaluating fit indices, including the chi-square (χ^2) statistic, Comparative Fit Index (CFI), and Root Mean Square Error of Approximation (RMSEA). Subsequently, path coefficients was derived for both the direct and indirect effects of each independent variable on the dependent variable from the model. The squared path coefficients for the direct and indirect paths estimated the respective direct and indirect contribution degrees of each independent variable to the dependent variable. The aggregate of these direct and indirect contribution degrees constitutes the total contribution degree, or relative contribution.

2.6 Validation of phenology "Saturation effect"

To determine if there was a temperature saturation effect on vegetation phenology, we initially assumed a logistic growth relationship between phenology and temperature. We then extracted phenological information from all vegetation pixels across the country and plotted scatter diagrams of phenology versus pre-season temperature. Next, we fitted logistic growth curves to these scatter plots and evaluated the assumption using the goodness-of-fit metrics p-value and R^2. Subsequently, we applied the same logistic curve to constrain the phenology of urban and suburban vegetation in 293 different cities against their pre-season temperatures, testing whether the phenological response to temperature in urban areas also follows a logistic growth pattern. Subsequently, we replaced the pre-season temperature with

https://doi.org/10.5194/egusphere-2026-241
Preprint. Discussion started: 4 March 2026

the background temperature LST to determine how the phenological saturation effect is regulated by the background temperature.

3. Results

3.1 Spatial distribution of urban-rural phenological differences

Among the 293 cities analyzed, 84% (N=246) exhibited an advanced SOS in urban areas compared to rural regions, while 82% (N=241) experienced a delayed EOS (Figure S3). Spatially, cities located in high-latitude regions generally demonstrated more negative ΔSOS values than those in low-latitude regions (Figure 2), indicating a stronger impact of urban warming on SOS in North and West China (Figure 2a, b). This pattern aligned with the conventional understanding of earlier SOS in colder regions. In addition, it seems that the cities in the coastal provinces have higher ΔSOS than the other regions (Figure 2).

A strong positive correlation was observed between ΔSOS and rural rate of SOS change ($R_{t\text{-}SOS}$), suggesting that cities with more negative $R_{t\text{-}SOS}$ values exhibit larger urban-rural disparities (Figure 3). It is noteworthy that cities with lower temperatures tended to have more negative $R_{t\text{-}SOS}$ and ΔSOS distributions.

ΔEOS exhibited an increasing trend with latitude gradient (Figure 2), with northern cities displaying more positive ΔEOS values, indicating a delayed autumn phenology (Figure 2c, d). In contrast, the majority of cities in southern regions demonstrated negative ΔEOS values, signifying an advancement in autumn phenology. Besides, cities in the coastal provinces also had higher ΔEOS.

Similarly, when ΔEOS was analyzed in relation to rural rate of EOS change ($R_{t\text{-}EOS}$), a positive correlation was observed. Positive and negative ΔEOS values were predominantly found in cold and warm regions, respectively (Figure 3). Moreover, as $\Delta EOS > 0$, both the absolute value of ΔEOS and $\Delta R_{t\text{-}EOS}$ increased with temperature, while for $\Delta EOS < 0$, the absolute value of ΔEOS and $\Delta R_{t\text{-}EOS}$ decreased with temperature.

https://doi.org/10.5194/egusphere-2026-241
Preprint. Discussion started: 4 March 2026

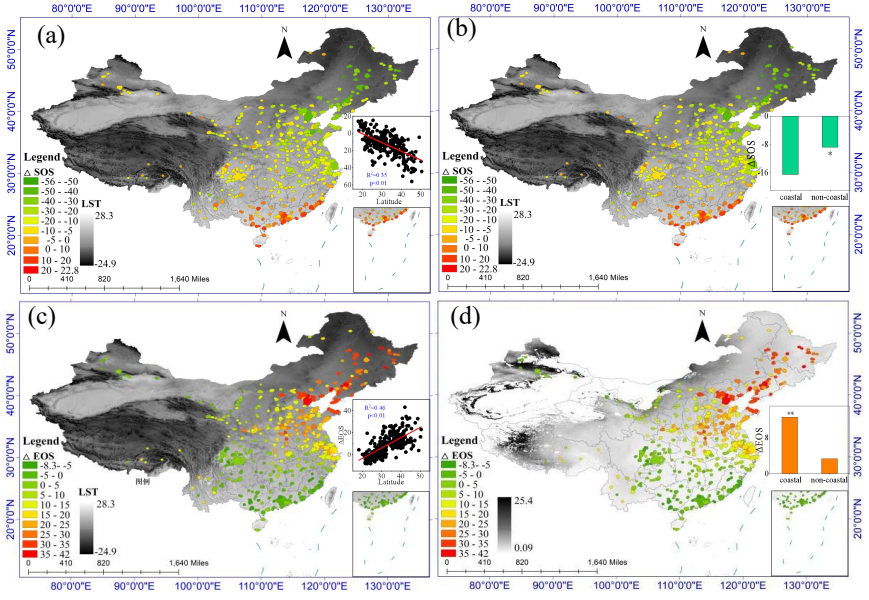

Figure 2. The spatial distribution of urban-rural disparities for SOS (ΔSOS) (a and b), EOS (ΔEOS) (c and d) was analyzed across mainland China. T (a, c) and AI (b, d) were represented in black-and-white range for the entire continent, and the data in these figures reflected the 10-year mean from 2010 to 2020 for each city. The inset figure shown in (a, c) depicts the latitude and longitude corresponding to ΔSOS and ΔEOS, while the inset figure shown in (b, d) compares ΔSOS and ΔEOS in coastal provinces with those in non-coastal provinces. The map, generated using ArcGIS – version10.2(https://www.esri.com/about/newsroom/arcwatch/the-best-of-arcgis-10-2/), features administrative boundaries sourced from the Ministry of Civil Affairs of the People's Republic of China (http://xzqh.mca.gov.cn/map). Source: Esri, TomTom, FAO, USGS, and the GIS User Community; Ministry of Civil Affairs of the People's Republic of China | Powered by Esri.

https://doi.org/10.5194/egusphere-2026-241
Preprint. Discussion started: 4 March 2026

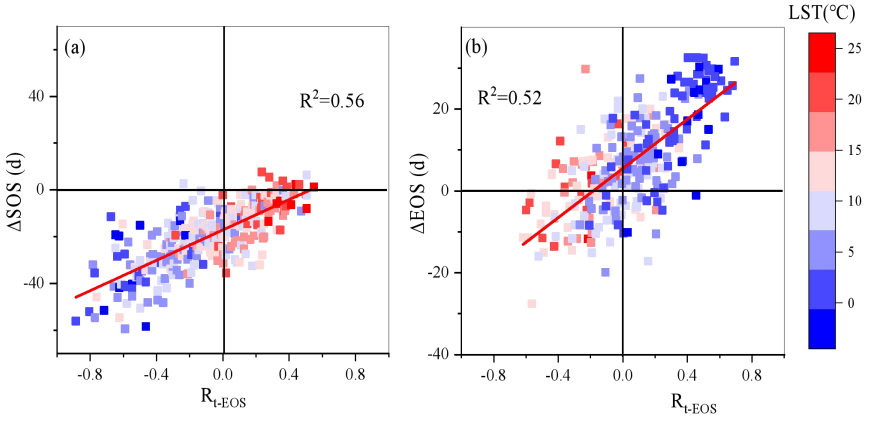

Figure 3. The phenology sensitivity was fitted to its urban-rural difference. The LST of each city was also presented by the red-blue ribbon.

3.2 phenology response to LST

As we compared urban and rural regions, logistic trends was observed for both SOS and EOS in relation to LST(Figure 4). In urban areas where LST was below 12℃, the SOS occurred notably earlier compared to rural regions, while urban areas exhibited a delayed EOS when LST was below 18.5℃. As LST decreased, the SOS stabilized at 101.3 days for urban regions and 129.7 days for rural regions, while the EOS stabilized at 321.3 days for urban areas and 310.8 days for rural areas. Conversely, when LST exceeded 12℃ or 18.5℃, the differences in SOS and EOS between urban and rural areas were not significant and sometimes even reversed (Figure 4a,b). As LST increased, the urban and rural SOS stabilized at 71.7 days (Figure 4a), and the urban and rural EOS stabilized at 327.4 days and 332.4 days, respectively. Fitting curve of ΔSOS and ΔEOS with LST revealed a positive and negative relationship, respectively, intersecting at LST=18℃ and 18.5℃, indicating a shift in SOS and EOS dynamics with increasing temperatures beyond these thresholds.

https://doi.org/10.5194/egusphere-2026-241
Preprint. Discussion started: 4 March 2026

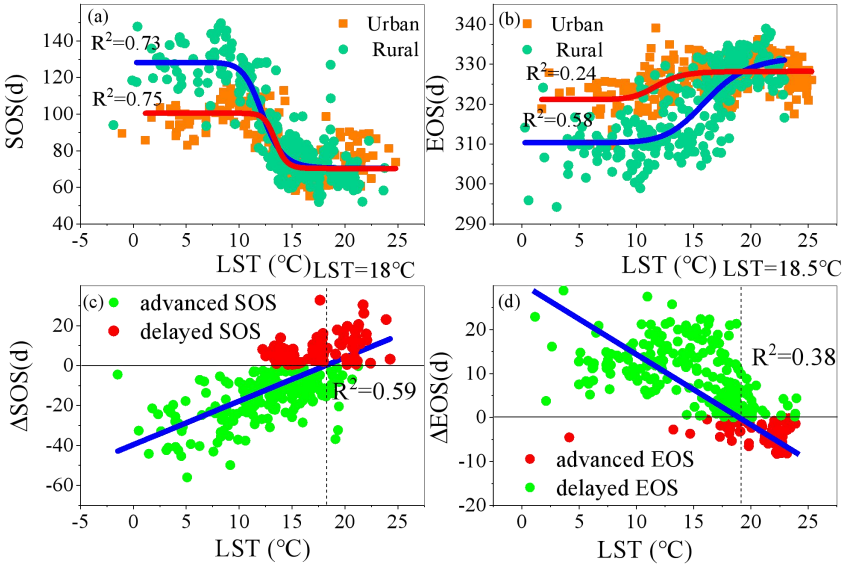

334

335 Figure 4. Relationship between background temperature (LST) and phenology (SOS
336 and EOS) across the urban-rural regions (a, b) from 2010 to 2020, and the relation
337 between ΔSOS and ΔEOS with the LST (c,d).

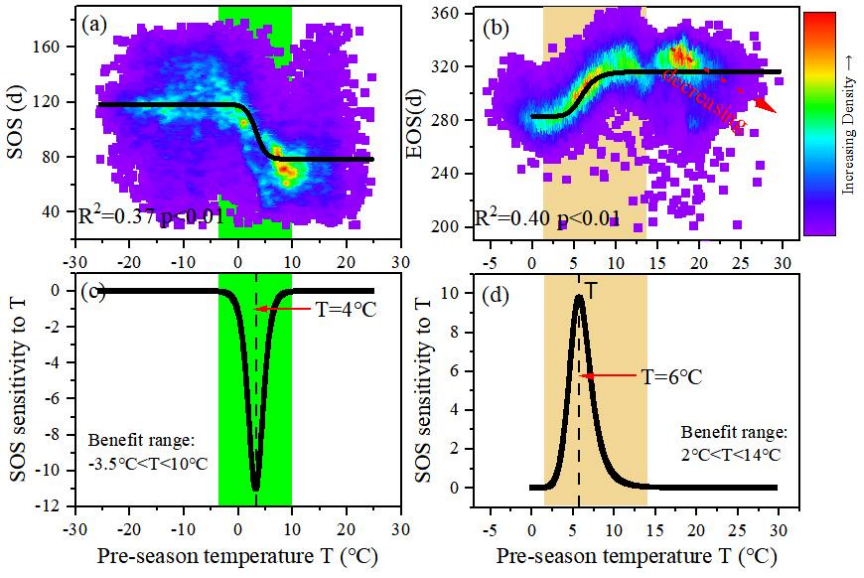

338

339 Figure 5. The relationship between preseason temperature (T) and SOS/EOS (a, b) as
340 well as their First-order derivatives (implying the phenology sensitivity to T) of the
341 fitting curve.

https://doi.org/10.5194/egusphere-2026-241
Preprint. Discussion started: 4 March 2026

To determine whether the temperature sensitivity influenced the logistic trends of phenology with LST, we conducted a nationwide fitting of phenology to T and also derived logistic curves for SOS and EOS (Figure 5). The first-order derivatives of the fitting curve that represented the phenology sensitivity to T revealed warming benefits on SOS and EOS, ranging from -3.5℃ to 10℃ and 2.0 to 13.5℃, respectively. The highest sensitivity was observed at T=4℃ for SOS and T=6℃ for EOS. Notably, a decreasing trend for EOS was observed when T>15℃, corresponding to the advanced EOS when T > 18.5℃ (Figure 5d).

To assess the temperature sensitivity of phenological variations between urban and rural settings across vegetation types, we established regression models for ΔSOS, ΔEOS, and LST for each type (Figure 6). Findings revealed that shrublands had the highest temperature sensitivity for both metrics, whereas CF displayed the lowest. The temperature response of MF and BF showed no significant variation.

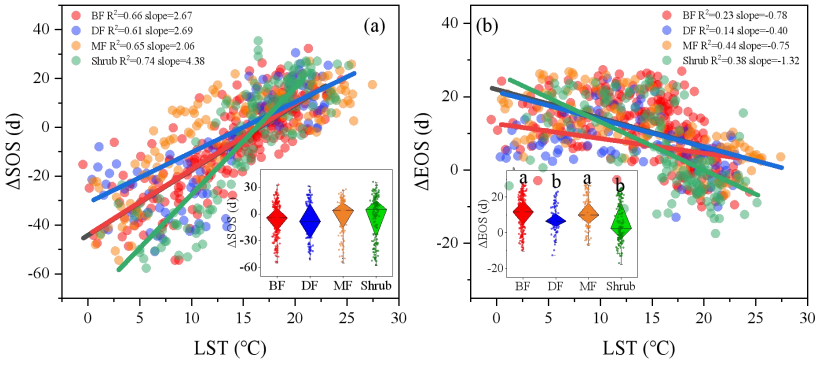

Figure 6. The relation between ΔSOS and ΔEOS with the LST across the 293 cities for different vegetation types, insert figures presented the comparison of averaged phenology difference across the 293 cities. BF: Broad-leaf forest, CF: Coniferous forest, MF: Mixed forest, Shrubs: Bush wood.

3.3 Quantify the LST determined phenology sensitivity

In order to obtain LST determined phenology sensitivity, the T in the first-order derivatives curves showed in Figure 5c, d was translated to LST considering the strong correlation between T and LST (Figure S4). Based on the derived curves, three

https://doi.org/10.5194/egusphere-2026-241
Preprint. Discussion started: 4 March 2026

possible scenarios for SOS and EOS sensitivity during urbanization across the mainland was observed (Figure 7).

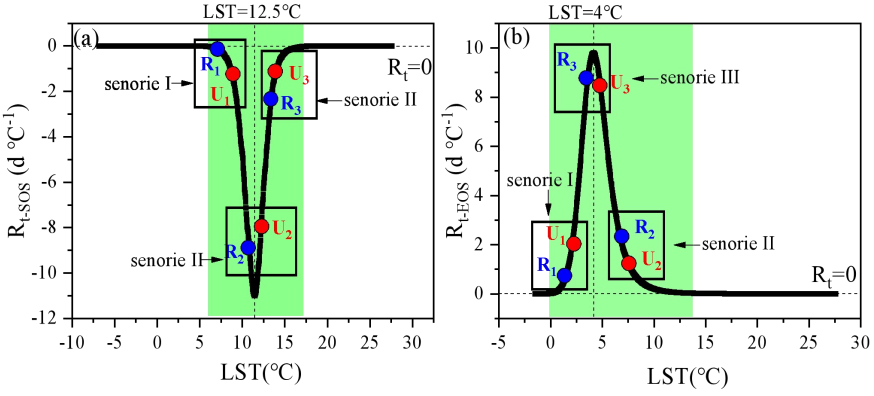

Figure 7. Schematic diagram for the three senories that likely occurred in the urban (red dots) and rural regions (blue dots) for SOS (I: LST_{R1} <LST_{U1}<12.5℃; II: 12.5℃<LST_{R2}<LST_{U2}; III:LST_{R3}<12.5℃<LST_{U3}) and EOS (I: LST_{R1} <LST_{U1}<4℃; II: 4℃<LST_{R2}<LST_{U2}; III:LST_{R3}<4℃<LST_{U3}).

Senories I: when LST was less than 12.5℃ (4℃) for SOS (EOS), an increased LST was associated with heightened temperature sensitivity, resulting in urban regions (U_1) exhibiting higher sensitivity than rural regions (R_1) (Figure 5).;

Senories II: when LST exceeded 12.5℃ (4℃) for SOS (EOS), there was a weakened temperature sensitivity as LST increased, leading to urban regions (U_2) demonstrating higher sensitivity than rural regions (R_2) (Figure 5).

Senories III: when urban LST surpassed 12.5℃ (4℃) while rural LST remained below 12.5℃ (4℃), the difference in sensitivity between urban and rural regions was inconclusive.

3.4 phenology response to aridity

When the phenological responses were fitted to the AI, $R_{t\text{-}SOS}$ and ΔSOS was positive related to AI (Figure 8). It is noted that when AI<1.7, there was a decrease in absolute $R_{t\text{-}SOS}$ with increasing AI, indicating that heightened aridity weakened the temperature sensitivity of SOS. Conversely, when AI>1.7, most urban areas exhibited positive $R_{t\text{-}SOS}$ (resulting in delayed SOS), with higher AI values corresponding to

https://doi.org/10.5194/egusphere-2026-241
Preprint. Discussion started: 4 March 2026

greater $R_{t\text{-}SOS}$, suggesting that severe drought conditions passively delay the onset of SOS.

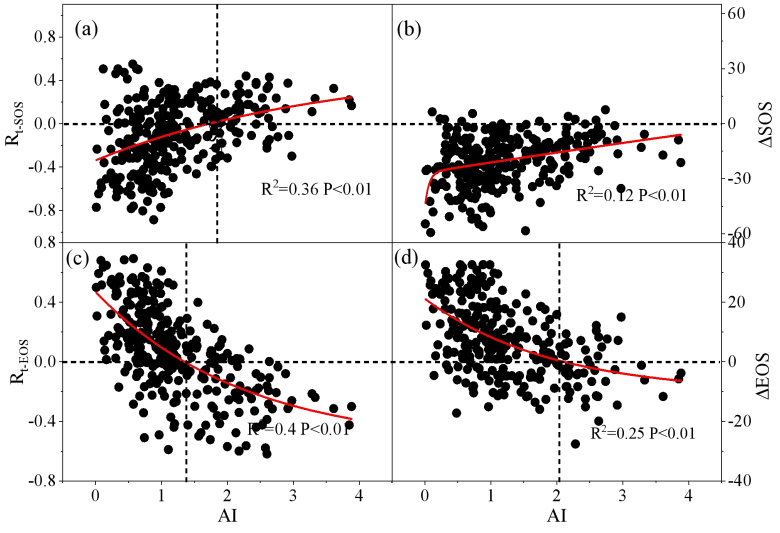

Figure 8. The AI determined phenology sensitivity and urban-rural difference

While $R_{t\text{-}EOS}$ and ΔEOS was fitted against AI, a negative relation was observed. For $R_{t\text{-}EOS}$, when AI < 1.4, most of the $R_{t\text{-}EOS}$ was positive, and decreased with AI, i.e., the enhanced drought will offset the benefit of urban warming on the delayed EOS. When AI>1.4, most cities shared a negative $R_{t\text{-}EOS}$, and the higher of AI, the more negative of the $R_{t\text{-}EOS}$. I.e., extremely drought will lead to passive warming effects on EOS. It is noted that the negative ΔEOS tended to appeared when AI >2.

AI has been observed to advance Δ SOS and hasten Δ EOS across 293 cities, with this pattern holding true for all four vegetation types (Figure 9). Notably, Δ SOS in CF showed less sensitivity to AI influences than the other vegetation types. Both BF and MF demonstrated lower sensitivities to AI for both Δ SOS and Δ EOS, as compared to shrublands.

https://doi.org/10.5194/egusphere-2026-241
Preprint. Discussion started: 4 March 2026

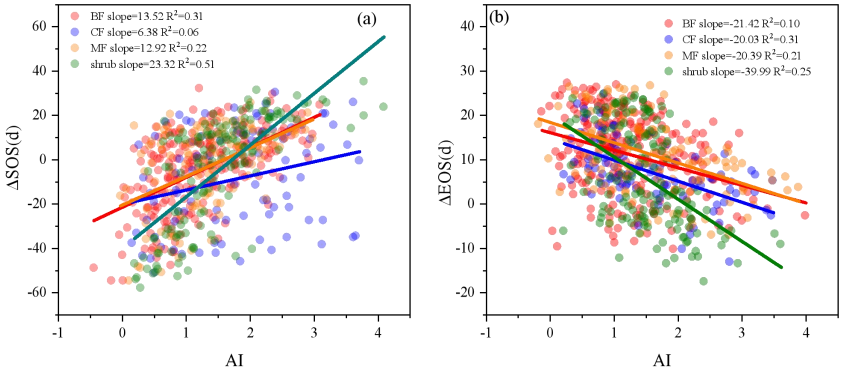

401

402 Figure 9. The AI determined phenology sensitivity and urban-rural difference for
403 different vegetation types.

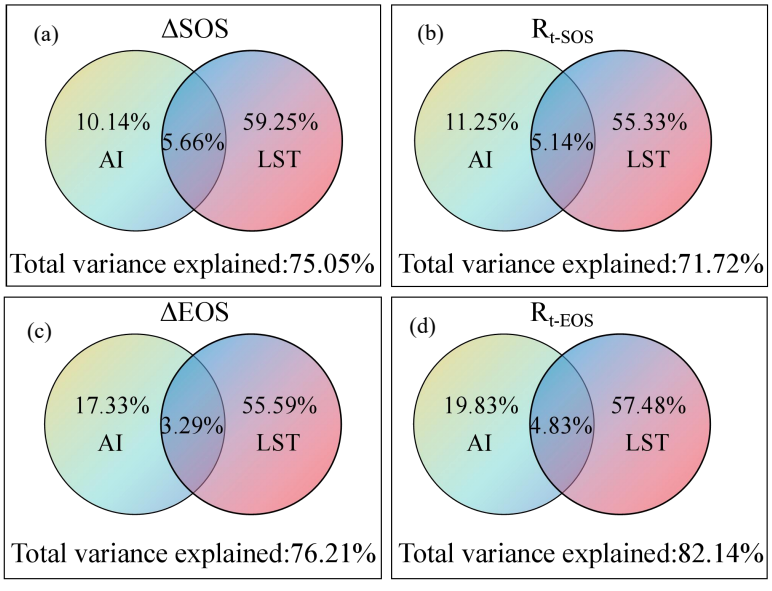

404

405 Figure 10. Venn diagrams illustrating the relative contribution of AI and LST to ΔSOS,
406 ΔEOS, $R_{t\text{-}SOS}$, $R_{t\text{-}EOS}$ across 293 cities in China. Each number in the panel indicates
407 that relative percentage explained by the combined factors.

408 The Venn diagram revealed that AI and LST explained 75.05%, 71.72%, 76.21%,
409 82.14% for ΔSOS, ΔEOS, $R_{t\text{-}SOS}$, $R_{t\text{-}EOS}$ respectively (Figure 10), and LST always had
410 more contributions for these phenology indicators. Besides, the interaction effect of
411 LST and AI ranged from 3.29%-5.66%.

https://doi.org/10.5194/egusphere-2026-241
Preprint. Discussion started: 4 March 2026

4. Discussion

4.1 Overall urbanization effects on plant phenology in China

In this study, the impact of urbanization on plant phenology across 293 cities in China was assessed. Our findings demonstrated a consistent advancement of SOS and delay of EOS in urban areas compared to rural regions in most of the studied cities (Figure S1), as argued in the previous studies(Jeonget et al., 2019; Meng et al., 2020; Qiu et al., 2020; Zhou et al., 2016). Notably, the urban warming effect on plant phenology was predominantly observed within a 10-km radius from the city centers (Figure S3), validating our definition of rural areas as those located over 20-km from the city centers.

Spatially, variations in ΔSOS and ΔEOS progressed from the south towards the north of China, mirroring the land surface temperature (LST) distribution across the continent (Figure 2). This aligns with previous research suggesting that the northern regions experience greater shifts in plant phenology than southern regions(Meng et al., 2020; Jia et al., 2021). Additional analysis showed that cities in the coastal provinces enjoyed more pronounced warming benefits compared to inland cities (Figure 2). Moreover, a strong correlation was found between delta SOS (ΔSOS), delta EOS (ΔEOS), and temperature sensitivity indicators ($R_{t\text{-}SOS}$ and $R_{t\text{-}EOS}$), as well as LST and AI (Figure 3). Thus, the expected impact of the background temperature and and aridity on the phenology response across the 293 cites was confirmed.

It is noted that the pattern of urban warming's benefit on the vegetation phenology was consistent among the four vegetation types (Figure S2). This consistency could be attributed to the ecological convergence for plants coexist in the same habitation(Wang et al., 2016), and within-spring warming have potential to intensify this phenological synchrony among different species(Wang et al., 2016).

https://doi.org/10.5194/egusphere-2026-241
Preprint. Discussion started: 4 March 2026

4.2 Background temperature related phenological response variance

When we quantified phenological responses to temperature, we expected a logistic growth model to fit both the SOS and EOS with rising temperatures (Figure 5). Interestingly, in urban areas, the growth rate for SOS/EOS began to plateau when temperatures exceeded 4℃/6℃ respectively (Figure 5). Taking into account the significant correlation between LST and T (Figure S4), we could also anticipate a diminished sensitivity in phenology with higher LST (Figure 7). These findings lend credibility to the "saturation" effect hypothesis, suggesting that the accelerating influence of warmth on vegetation phenology reported in earlier studies has its limits (Badeck et al., 2004; Li et al., 2021). Indeed, plants in the southern region exhibit not just a dampened phenological response but also a decelerated growth rate when faced with increasing temperatures(Li et al., 2021; Buntgen et al., 2019). Collectively, these results underscore the importance of considering non-linear and threshold-based models when predicting phenological responses under scenarios of continuous environmental warming, especially in urban settings.

The observation of temperature saturation for the SOS in our study likely stems from the chilling requirements for vernalization(Kim et al., 2009; Hanninen et al., 2019). Typically, following a halt in growth during the early fall, vegetation needs to undergo a period of exposure to low chilling temperatures to exit dormancy. However, Nonetheless, when ambient temperatures are relatively high, these chilling requirements may not be met(Meng et al., 2020), thus diminished phenological sensitivity in warmer territories (Figure 2,3). Moreover, an earlier onset of greening increased the risk of damage from freezing events, posing a survival threat to the plants(Duan et al., 2011; Wang et al., 2015).This phenomenon had led to a delayed SOS in approximately 16% of the cities under study, predominantly located in lower latitude areas (most in the low latitude regions, Figure 4).

Regarding the EOS, a moderate increase in temperature could enhance the activities of photosynthetic enzymes(Shi et al., 2014), slow down the degradation of chlorophyll(Fracheboud et al., 2009), reduce the risk of frost exposure in autumn, and

https://doi.org/10.5194/egusphere-2026-241
Preprint. Discussion started: 4 March 2026

increase the potential for growth and photosynthetic consumption, ultimately promoting the extension of the growing season. While the benefits of increased temperature can be offset by the negative impact of heat waves and droughts that result from higher LST. These passive feedback loops can cause widespread leaf senescence and even crown defoliation50-51(Estiarte & Penuelas, 2015; Pollastrini et al., 2017), potentially negating the benefits of an earlier onset of the growing season. In fact, when T>15 ℃, EOS tends to be reduced, with an increased sensitivity to temperature changes (Figure 5b).

While even the existence of "saturation" effects, the lower background temperatures was not necessarily correspond to higher phenological sensitivity (Figure 4b, c). For SOS, when T < 4℃, the phenological sensitivity was approaching zero with decreased T (Figure 4c), which led to a stable SOS of 120d (Figure 5a,c). In fact, phenological events such as bud burst could not be triggered when high forcing temperatures threshold (cumulative temperature) was not fully provided46(Hanninen et al., 2019). For EOS, when T>6℃, the increased T sensitivity will produce more EOS advancement in the warmer regions. This could be related to the associated with the increase of abscisic acid synthesis induced by low temperature, which accelerated the progress of defoliation.

In our study, when we quantify the phenology sensitivity response to the LST, we found that the phenological sensitivity in response the LST was not unidirectional, but fluctuant, for both SOS and EOS. For SOS, the positive phenological response in the urban regions was validated 6<LST<17.5℃ (Figure 5). However, when LST<12.5℃, warming regions would have higher urban-rural difference of $\Delta R_{t\text{-}SOS}$, which contradicted the weakened urban-rural difference of $\Delta R_{t\text{-}SOS}$ raised in the previous study(Meng et al., 2020). For EOS, the warming benefits only occurred when 0<LST<18℃. Moreover, the weakened sensitivity only in the LST interval of LST>4℃. The conclusions of weakened $\Delta R_{t\text{-}SOS}$ and $\Delta R_{t\text{-}EOS}$ in the USA could attributed to their LST ranges was mostly falling in the ranges of 8℃-22℃(Meng et al., 2020).

https://doi.org/10.5194/egusphere-2026-241
Preprint. Discussion started: 4 March 2026

4.3 AI related phenological response variance

Except for the LST, the AI related spatial variation of ΔSOS and ΔEOS was also validated. Spatially, the coastal cities experienced more benefits from the urban warming(Figure 2). Statistically, both $R_{t\text{-}SOS}$ and ΔSOS increased with AI, while both $R_{t\text{-}SOS}$ and ΔSOS decreased with AI. Consequently, AI explained 10.14% and 17.33% variation dependently for the spatial distribution of ΔSOS and ΔEOS. These results highlight that the warming benefits on the vegetation phenology will be weaken in those drought dominated regions. In fact, the delayed SOS was already proved in the previous studies(Ji et al., 2021; Yu et al., 2023).

It has been suggested that under the condition of water deficit, roots of plants would produce chemical signals such as abscisic acid and cytokinins, which may limit leaf growth(Knauer et al., 2017). Urbanization have potential to intensify the drought condition(Zhang et al., 2019), thus weaken and even reverse the warming benefits. Besides, in water-stressed region, temperatures are already close to the optimum for photosynthesis, thus less benefits will be expected(Penuelas et al., 2004). The weakened temperature sensitivity in drought cities will certainly led to less extension of growth season.

While it is noted that the influence of AI on the autumn phenology response was higher than that on the spring phenology response (Figure 10). During spring leaf development, plants may use water stored in their bodies to support the growth of new leaves(Shi et al., 2023). Evidence had been proved by the synchronous in plant water storage and leaf sprout for the boreal and temperate forests(Tian et al., 2018). In this case, the external water supply may have relatively little demand on the plant during the leaf development period, especially in some wetter areas. Comparatively, In summer and autumn, the transpiration of plants is larger, and the demand for water is strong(Wu et al., 2022), so the influence of drought degree on plant phenology will be more prominent.

https://doi.org/10.5194/egusphere-2026-241
Preprint. Discussion started: 4 March 2026

4.4 Phenological response variation among different vetation type

In the response to variations in temperature and the Aridity Index (AI), significant differences in sensitivity are observed among different vegetation types. Shrub species exhibit heightened sensitivity, whereas coniferous tree species display relative insensitivity. These discrepancies reflect the influence of functional traits on the phenology of vegetation. Studies on forests in northern China indicate that broadleaf forests and mixed forests are the most sensitive to climatic factors, followed by coniferous forests(Zheng et al., 2022). Broadleaf tree species, with their higher demands for light and temperature(Wu et al., 2015), are more likely to benefit from warming temperatures, thereby promoting their growth(Malla et al., 2023). However, as AI increases, broadleaf species face more severe water limitations. Coniferous species, due to their drought-resistant characteristics such as needle morphology, stomatal recess, and weaker water transport capacity, exhibit lower sensitivity to changes in AI, which limits the potential positive impact of warming on their phenology. In contrast, the extensive resource utilization strategy of shrub species may be the primary reason for their high sensitivity to climate change(Xiong et al., 2024).

5. Conclusion

Our study utilized remote sensing data to investigate the impact of urbanization on vegetation phenology in 293 cities from 2010 to 2020. The advanced SOS and delayed EOS was validated in most cities due to urban warming effects, however, with different sensitivity due to the spatial variance of LST and AI.

The assumption that the “saturation effect” of plant phenological response to warming can explain the gradually reduced urban SOS and EOS shift in warming regions when LST<12.5 ℃ and LST>4 ℃ respectively. Otherwise, warmer regions would experience much more benefits due to urban warming. The warming benefit would valid only when 3.5℃ <LST<17.5℃, and 0℃<LST<18℃, otherwise, the

https://doi.org/10.5194/egusphere-2026-241
Preprint. Discussion started: 4 March 2026

phenology sensitivity will approach 0, and moreover, extremely high temperatures has the potential to reverse the warming benefits, leading to weakly delayed or even advanced EOS in warming regions.

Drought also has potential to weaken the urban warming benefit on SOS and EOS, which leading to higher ΔSOS and ΔEOS in the coastal cities. When AI<1.4 or AI>2.0, increased AI will weaken the warming benefits for SOS and EOS, while when 1.4<AI<2.0, warming benefits was even reversed for SOS and EOS.

6. Author contributions: CRediT

Cui Shufen: Conceptualization, Methodology; Zhang Zhenzhen: Data curation, Writing- Original draft preparation; Zhang Yongqi: Visualization, Investigation; Sun Liheng, Wu Chaofan and Lin Xingwen: Supervision; Zhang Zhaoyang, Chen Yuanjian and Wen Qingqing: Software, Validation.

7. Data availability statement

The data that support the findings of this study are available in those public domain resources that listed in the table 1.

8. Conflict of Interest

The authors declared that the research was conducted in the absence of any commercial or financial relationships that could be construed as a potential conflict of interest.

Founding

This study was supported by “Department of science and technology of Zhejiang Province in China, “Pioneer” and “Bellwethers” R & D projects, grant number 2022C03119”.

https://doi.org/10.5194/egusphere-2026-241
Preprint. Discussion started: 4 March 2026

References

Badeck, F.-W., Bondeau, A., Böttcher, K., Doktor, D., Lucht, W., Schaber, J. and Sitch, S. (2004). Responses of spring phenology to climate change. New Phytologist. **162,** 295-309.

Buyantuyev, A., & Wu, J. (2012). Urbanization diversifies land surface phenology in arid environments: Interactions among vegetation, climatic variation, and land use pattern in the Phoenix metropolitan region, USA. Landscape and Urban Planning. **105,** 149-159.

Büntgen, U., Krusic, P.J., Piermattei, A., Coomes, D.A., Esper, J., Myglan, V.S., Kirdyanov, A.V., Camarero, J.J., Crivellaro, A., Körner, C. (2019). Limited capacity of tree growth to mitigate the global greenhouse effect under predicted warming. Nature Communication. **10,** 2171.

Cai, Z., Jönsson, P., Jin, H., & Eklundh, L. (2017). Performance of smoothing methods for reconstructing NDVI time-Series and estimating vegetation phenology from MODIS Data. Remote Sensing. **9,** 1271.

Čehulić, I., Sever, K., Katičić Bogdan, I., Jazbec, A., Škvorc, Ž., & Bogdan, S. (2019). Drought Impact on Leaf Phenology and Spring Frost Susceptibility in a Quercus robur L. Provenance Trial. Forests. **10,** 50.

Chmielewski, F.-M., & Rötzer, T. (2001). Response of tree phenology to climate change across Europe. Agricultural and Forest Meteorology. **108,** 101-112.

Cong, N., Piao, S., Chen, A., Wang, X., Lin, X., Chen, S., Han, S., Zhou, G., Zhang, X. (2012). Spring vegetation green-up date in China inferred from SPOT NDVI data: A multiple model analysis. Agricultural and Forest Meteorology. **165,** 104-113.

Dallimer, M., Tang, Z., Gaston, K. J., & Davies, Z. G. (2016). The extent of shifts in vegetation phenology between rural and urban areas within a human-dominated region. Ecology and Evolution. **6,** 1942-1953.

Ding, H., Xu, L., Elmore, A. J., & Shi, Y. (2020). Vegetation phenology influenced by rapid urbanization of The Yangtze Delta region. Remote Sensing. **12,** 1783.

Duan, J., Zhang, Q.-B., Lv, L., & Zhang, C. (2011). Regional-scale winter-spring

https://doi.org/10.5194/egusphere-2026-241
Preprint. Discussion started: 4 March 2026

temperature variability and chilling damage dynamics over the past two centuries in southeastern China. Climate Dynamics. **39,** 919-928.

Eidt, D. C., & Little, C. J. C. E. (1968). Insect control by artificially prolonging plant dormancy — a new approach. The Canadian Entomologist. **100,** 1278-1279.

Estiarte, M., & Penuelas, J. (2015). Alteration of the phenology of leaf senescence and fall in winter deciduous species by climate change: effects on nutrient proficiency. Global Change Biology. **21,** 1005-1017.

Fan, J., He, H., Hu, T., Zhang, P., Yu, X., & Zhou, Y. (2019). Estimation of landscape pattern changes in BRICS from 1992 to 2013 using DMSP-OLS NTL images. Journal of the Indian Society of Remote Sensing. **47,** 725-735.

Fracheboud, Y., Luquez, V., Bjorken, L., Sjodin, A., Tuominen, H., & Jansson, S. (2009). The control of autumn senescence in European aspen. Plant Physiology. **149,** 1982-1991.

Gazal, R., White, M. A., Gillies, R., Rodemaker, E. L. I., Sparrow, E., & Gordon, L. (2008). GLOBE students, teachers, and scientists demonstrate variable differences between urban and rural leaf phenology. Global Change Biology. **14,** 1568-1580 .

Ge, W., Han, J., Zhang, D., & Wang, F. (2021). Divergent impacts of droughts on vegetation phenology and productivity in the Yungui Plateau, southwest China. Ecological Indicators. **127**, 107743.

Gow, L. J., Barrett, D. J., Renzullo, L. J., Phinn, S. R., & O'Grady, A. P. (2016). Characterising groundwater use by vegetation using a surface energy balance model and satellite observations of land surface temperature. Environmental Modelling & Software. **80,** 66-82.

Hanninen, H., Kramer, K., Tanino, K., Zhang, R., Wu, J., & Fu, Y. H. (2019). Experiments are necessary in process-based tree phenology modelling. Trends in Plant Science. **24,** 199-209.

He, C., Gao, B., Huang, Q., Ma, Q., & Dou, Y. (2017). Environmental degradation in the urban areas of China: Evidence from multi-source remote sensing data. Remote Sensing of Environment. **193,** 65-75.

Jeong, S. J., Park, H., Ho, C. H., & Kim, J. (2019). Impact of urbanization on spring and

https://doi.org/10.5194/egusphere-2026-241
Preprint. Discussion started: 4 March 2026

631 autumn phenology of deciduous trees in the Seoul Capital Area, South Korea.
632 International Journal of Biometeorology. **63,** 627-637.
633 Ji, S., Ren, S., Li, Y., Dong, J., Wang, L., Quan, Q., & Liu, J. (2021). Diverse responses of
634 spring phenology to preseason drought and warming under different biomes in the
635 North China Plain. Science of the Total Environment. **766,** 144437.
636 Jia, W., Zhao, S., Zhang, X., Liu, S., Henebry, G. M., & Liu, L. (2021). Urbanization
637 imprint on land surface phenology: The urban-rural gradient analysis for Chinese
638 cities. Global Chang Biology. **27,** 2895-2904.
639 Kang, X., Hao, Y., Cui, X., Chen, H., Huang, S., Du, Y., Li, W., Kardol, P., Xiao, X., Cui,
640 L. (2016). Variability and changes in climate, phenology, and gross primary
641 production of an Alpine wetland ecosystem. Remote Sensing. **8,** 391.
642 Ketola, T., & Kristensen, T. N. (2017). Experimental approaches for testing if tolerance
643 curves are useful for predicting fitness in fluctuating environments. Frontiers in
644 Ecology and Evolution. **5,** 129.
645 Kim, D. H., Doyle, M. R., Sung, S., & Amasino, R. M. (2009). Vernalization: winter and
646 the timing of flowering in plants. Annual Review of Cell and Developmental Biology.
647 **25,** 277-299.
648 Knauer, J., Zaehle, S., Reichstein, M., Medlyn, B. E., Forkel, M., Hagemann, S., & Werner,
649 C. (2017). The response of ecosystem water-use efficiency to rising atmospheric CO
650 2 concentrations: sensitivity and large-scale biogeochemical implications. New
651 Phytologist. **213,** 1654-1666.
652 Li, K., Wang, C., Sun, Q., Rong, G., Tong, Z., Liu, X., & Zhang, J. (2021). Spring
653 phenological sensitivity to climate Change in the northern hemisphere:
654 comprehensive evaluation and driving force analysis. Remote Sensing. **13,** 1972.
655 Malla, R., Neupane, P. R., & Köhl, M. (2023). Climate change impacts: Vegetation shift of
656 broad-leaved and coniferous forests. Trees, Forests and People. **14,** 100457 .
657 Mathur S., Agrawal D., Jajoo A. (2014). Photosynthesis: response to high temperature
658 stress. Journal of Photochemistry and Photobiology B: Biology. **137,** 116-126.
659 Mcadam, B. S. A. M. J. P. P. (2013). Abscisic acid mediates a divergence in the drought
660 response of two conifers. Plant physiology. **162,** 1370-1377.

https://doi.org/10.5194/egusphere-2026-241
Preprint. Discussion started: 4 March 2026

661 Meng, L., Mao, J., Zhou, Y., Richardson, A.D., Lee, X., Thornton, P.E., Ricciuto, D.M., Li,
662 X., Dai, Y., Shi, X., Jia, G. (2020). Urban warming advances spring phenology but
663 reduces the response of phenology to temperature in the conterminous United States.
664 Proceedings of the National Academy of Sciences of the United States of America.
665 **117,** 4228-4233.
666 Pablos, M., Martínez-Fernández, J., Piles, M., Sánchez, N., Vall-llossera, M., & Camps, A.
667 (2016). Multi-temporal evaluation of soil moisture and land surface temperature
668 dynamics using in situ and satellite observations. Remote Sensing. **8,** 587.
669 Peng, J., Wu, C., Zhang, X., Wang, X., & Gonsamo, A. (2019). Satellite detection of
670 cumulative and lagged effects of drought on autumn leaf senescence over the
671 Northern Hemisphere. Global Change Biology. **25,** 2174-2188.
672 Peng, S. (2020). 1-km monthly precipitation dataset for China (1901-2021). Retrieved
673 from: https://dx.doi.org/10.5281/zenodo.3185722.
674 Penuelas, J., Gordon, C., Llorens, L., Nielsen, T., Tietema, A., Beier, C., ... & Gorissen, A.
675 (2004). Nonintrusive field experiments show different plant responses to warming
676 and drought among sites, seasons, and species in a north–south European gradient.
677 Ecosystems. **7,** 598-612.
678 Piao, S., Fang, J., Zhou, L., Ciais, P., & Zhu, B.(2006). Variations in satellite-derived
679 phenology in China's temperate vegetation. Global Change Biology. **12,** 672-685.
680 Pollastrini, M., Nogales, A.G., Benavides, R., Bonal, D., Finer, L., Fotelli, M., Gessler, A.,
681 Grossiord, C., Radoglou, K., Strasser, R.J., Bussotti, F. (2017). Tree diversity affects
682 chlorophyll a fluorescence and other leaf traits of tree species in a boreal forest. Tree
683 Physiology. **37,** 199-208.
684 Pollastrini, M., Puletti, N., Selvi, F., Iacopetti, G., & Bussotti, F. (2019). Widespread
685 crown defoliation after a drought and heat wave in the forests of Tuscany (Central
686 Italy) and their recovery—A case study from summer 2017. Frontiers in Forests and
687 Global Change. **2**.
688 Qiao, Z., Tian, G., & Xiao, L. (2013). Diurnal and seasonal impacts of urbanization on the
689 urban thermal environment: A case study of Beijing using MODIS data. ISPRS
690 Journal of Photogrammetry and Remote Sensing. **85,** 93-101.

https://doi.org/10.5194/egusphere-2026-241
Preprint. Discussion started: 4 March 2026

691 Qiu, T., Song, C., & Li, J. (2017). Impacts of urbanization on vegetation phenology over
692 the past three decades in Shanghai. China. Remote17 Sensing. **9,** 970.
693 Qiu, T., Song, C., Zhang, Y., Liu, H., & Vose, J. M. (2020). Urbanization and climate
694 change jointly shift land surface phenology in the northern mid-latitude large cities.
695 Remote Sensing of Environment. **236,** 111477.
696 Rustad, L., Campbell, J., Marion, G., Norby, R., Mitchell, M., Hartley, A., Cornelissen, J.,
697 Gurevitch, J., Gcte, N. (2001). A meta-analysis of the response of soil respiration, net
698 nitrogen mineralization, and aboveground plant growth to experimental ecosystem
699 warming. Oecologia. **126,** 543–562.
700 Sage, R.F. and Kubien, D.S. (2007). The temperature response of C3 and C4
701 photosynthesis. Plant. Cell & Environment. **30,** 1086-1106.
702 Shi, C., Sun, G., Zhang, H., Xiao, B., Ze, B., Zhang, N., & Wu, N. (2014). Effects of
703 warming on chlorophyll degradation and carbohydrate accumulation of Alpine
704 herbaceous species during plant senescence on the Tibetan Plateau. PLoS One. **9,**
705 e107874.
706 Shi, W., Li, J., Zhan, H., Yu, L., Wang, C., & Wang, S. (2023). Relation between water
707 storage and photoassimilate accumulation of neosinocalamus affinis with phenology.
708 Forests. **14,** 531.
709 Tang, J. W., Korner, C., Muraoka, H., Piao, S. L., Shen, M. G., Thackeray, S. J., & Yang,
710 X. (2016). Emerging opportunities and challenges in phenology: a review. Ecosphere.
711 **7,** e01436.
712 Tian, F., Wigneron, J.-P., Ciais, P., Chave, J., Ogée, J., Peñuelas, J., Ræbild, A., Domec,
713 J.-C., Tong, X., Brandt, M., Mialon, A., Rodriguez-Fernandez, N., Tagesson, T.,
714 Al-Yaari, A., Kerr, Y., Chen, C., Myneni, R.B., Zhang, W., Ardö, J., Fensholt, R.
715 (2018). Coupling of ecosystem-scale plant water storage and leaf phenology observed
716 by satellite. Nature ecology & evolution. **2,** 1428-1435.
717 Wan, Z. (2008). New refinements and validation of the MODIS Land-Surface
718 Temperature/Emissivity products. Remote Sensing of Environment. **112**, 59-74 .
719 Wang, C., Cao, R., Chen, J., Rao, Y., & Tang, Y. (2015). Temperature sensitivity of spring
720 vegetation phenology correlates to within-spring warming speed over the Northern

https://doi.org/10.5194/egusphere-2026-241
Preprint. Discussion started: 4 March 2026

721 Hemisphere. Ecological Indicators. **50,** 62-68.
722 Wang, C., Tang, Y., & Chen, J. (2016). Plant phenological synchrony increases under rapid
723 within-spring warming. Scientific Reports. **6,** 25460.
724 Wang, Z., Ma, R., Zhao, M., Wang, F., Zhang, N., & Si, H. (2020). NO and ABA
725 interaction regulates tuber dormancy and sprouting in Potato. Frontiers in Plant
726 Science. **11,** 311.
727 White, M.A., De Beurs, K.M., Didan, K., Inouye, D.W., Richardson, A.D., Jensen, O.P.,
728 O'Keefe, J., Zhang, G., Nemani, R.R., Van Leeuwen, W.J.D., Brown, J.F., De Wit, A.,
729 Schaepman, M., Lin, X., Dettinger, M., Bailey, A.S., Kimball, J., Schwartz, M.D.,
730 Baldocchi, D.D., Lee, J.T., Lauenroth, W.K. (2009). Intercomparison, interpretation,
731 and assessment of spring phenology in North America estimated from remote sensing
732 for 1982-2006. Global Change Biology. **15,** 2335-2359 .
733 Wu, C., Peng, J., Ciais, P., Peñuelas, J., Wang, H., Beguería, S., ... & Ge, Q. (2022).
734 Increased drought effects on the phenology of autumn leaf senescence. Nature
735 Climate Change. **12,** 943-949.
736 Wu, D., Zhao, X., Liang, S., Zhou, T., Huang, K., Tang, B., & Zhao, W. (2015). Time-lag
737 effects of global vegetation responses to climate change. Global change biology. **21,**
738 3520-3531.
739 Xiong, X., Wu, H., Wei, X., & Jiang, M. (2024). Contrasting temperature and light
740 sensitivities of spring leaf phenology between understory shrubs and canopy trees:
741 Implications for phenological escape. Agricultural and Forest Meteorology. **355,**
742 110144.
743 Yao, R., Wang, L., Huang, X., Guo, X., Niu, Z., & Liu, H. (2017). Investigation of
744 Urbanization effects on land Surface phenology in Northeast China during
745 2001–2015. Remote Sensing. **9,** 66.
746 Yu, F., Price, K. P., Ellis, J., & Shi, P. (2003). Response of seasonal vegetation
747 development to climatic variations in eastern central Asia. Remote sensing of
748 environment. **87,** 42-54.
749 Yuan, M., Zhao, L., Lin, A., Wang, L., Li, Q., She, D., & Qu, S. (2020). Impacts of
750 preseason drought on vegetation spring phenology across the Northeast China

https://doi.org/10.5194/egusphere-2026-241
Preprint. Discussion started: 4 March 2026

751 Transect. Science of the Total Environment. **738,** 140297.
752 Zhang, X., Friedl, M. A., Schaaf, C. B., Strahler, A. H., & Schneider, A. (2004). The
753 footprint of urban climates on vegetation phenology. Geophysical Research Letters.
754 **31,** L12209.
755 Zhang, X., Friedl, M. A., & Schaaf, C. B. (2006). Global vegetation phenology from
756 Moderate Resolution Imaging Spectro radiometer (MODIS): Evaluation of global
757 patterns and comparison with in situ measurements. Journal of Geophysical Research:
758 Biogeosciences. **111**.
759 Zhang, X., Chen, N., Sheng, H., Ip, C., Yang, L., Chen, Y., ... & Niyogi, D. (2019). Urban
760 drought challenge to 2030 sustainable development goals. Science of the Total
761 Environment. **693,** 133536.
762 Zheng, W., Liu, Y., Yang, X., & Fan, W. (2022). Spatiotemporal variations of forest
763 vegetation phenology and its response to climate change in northeast China. Remote
764 Sensing. **14,** 2909.
765 Zhou, D., Zhao, S., Zhang, L., & Liu, S. (2016). Remotely sensed assessment of
766 urbanization effects on vegetation phenology in China's 32 major cities. Remote
767 Sensing of Environment. **176,** 272-281.
768